Texture-Integrated Classification of Urban Treed Areas in High-Resolution Color-Infrared Imagery

Yun Zhang

Abstract

Traditional multispectral classification methods have not provided satisfying results for treed area extraction from high-resolution digital imagery because trees are characterized not only by their spectral but also by their textural properties. Treed areas in urban regions are especially difficult to extract due to their small area. Many other urban objects, such as lawn and playgrounds, cause confusion because they display similar, even identical, spectral properties. In this study a texture integrated classification method is proposed. To effectively extract tree textural features and eliminate noise, an algorithm of conditional variance detection is developed, which consists of a directional variance detection and a local variance detection. This algorithm detects tree features with higher accuracy than common texture algorithms. By integrating the new algorithm with traditional multispectral classification, treed areas in urban regions can be extracted with sufficiently high accuracy. Application of the new approach in different urban areas indicates that the average accuracy of treed area extraction was increased from 67 percent, using a multispectral classification, to 96 percent, using the texture integrated classification.

Introduction

Inventory and mapping of urban treed areas is important for urban environment study and urban planning. Traditionally, urban treed areas are extracted and mapped through visual interpretation of aerial color-infrared images and fieldwork (Nowak *et al.*, 1996). Multispectral classification methods have been used to extract urban treed areas from digitized aerial images, but successful results have rarely been achieved because of the variety of spectral and textural properties of trees (Hildebrandt, 1996). Many studies on classification of medium-resolution satellite imagery (e.g., Landsat TM, SPOT) in urban or urban-rural areas demonstrated that treed areas, except large wooded areas within big parks and suburban areas, could not be extracted because of the lack of spatial resolution (Barnsley and Barr, 1996; Gao and Skillcorn, 1998). In some studies, urban treed areas were extracted by including texture information. The extracted treed areas could, however, not be separated from lawn areas (Gong and Howarth, 1990; Zhang, 1998a).

Numerous high-resolution airborne sensors have been developed. The world's first commercial high-resolution satellite imagery, IKONOS, has been available since the fall of 1999. However, the improvement of the spatial resolution does not automatically increase classification accuracy when conventional multispectral classification methods are used (Marceau *et al.*, 1994), because high spatial resolution increases spectral and spatial variation within individual classes. By analyzing intraclass local variances in images with different resolutions, Woodcock and Strahler (1987) suggested that, in urban and forested environments, techniques utilizing texture modelling were appropriate for images with a resolution of 10 to 30 m; Marceau *et al.* (1994) concluded that an average 10-m spatial resolution was optimal for spectral classification of a temperate forested environment, while higher spatial resolution did decrease the classification accuracy. To classify images in urban environments with a higher resolution (e.g., less than 5 m), new algorithms and tools considering textural information are consequently required. Such algorithms and tools are especially important for dealing with the problems arising from the rapid emergence of high-resolution imagery.

Many studies on extracting detailed tree information from high-resolution real or simulated images have utilized tree textural features in the extraction. For example, neural network (Dreyer, 1993), co-occurrence matrix (Anys *et al.*, 1994), valley following (Gougeon, 1995), semivariogram (St-Onge and Cavayas, 1997), threshold-based spatial clustering (Culvenor *et al.*, 1999), local maximum filtering (Wulder *et al.*, 2000), and local variance (Coops and Culvenor, 2000) were employed to identify tree textures. However, reliable texture extraction or successful tree recognition in real remote sensing data is difficult (Bruniquel-Pinel and Gastellu-Etchegorry, 1998; Pinz, 1999). Although some approaches worked well with high-resolution images containing near fully forested areas, the success rate reduced rapidly in the areas where man-made structures are located (St-Onge and Cavayas, 1997), especially in urban areas (Anys *et al.*, 1994).

To separate buildings from treed areas, digital surface models (DSMs) generated by airborne laser scanners were employed as main or auxiliary sources in some studies. For example, Hahn and Stätter (1998) extracted treed areas according to both the spectral information in airborne color-infrared images (0.5-m resolution) and the height information in laser DSMs. Brunn and Weidner (1997) used the geometric information of trees in a DSM to discriminate trees from buildings. Haala *et al.* (1998) extracted buildings and treed areas using laser DSMs and maps. However, airborne laser DSMs are currently expensive and not available for many cities. Using geometric information in DSMs, it is difficult to separate trees from buildings when they are close to each other. In addition, information on the location of buildings available in a map is not always current.

In this study, a simple but effective method is proposed to extract urban treed areas directly from high-resolution color-infrared images without using any auxiliary height information. This method integrates the textural and spectral information of

Photogrammetric Engineering & Remote Sensing
Vol. 67, No. 12, December 2001, pp. 1359–1365.

0099-1112/01/6712–1359$3.00/0

Department of Geodesy and Geomatics Engineering, University of New Brunswick, P.O. Box 4400, Fredericton, New Brunswick E3B 5A3, Canada (yunzhang@unb.ca).

trees in the classification. To effectively detect tree textures, a conditional texture detection algorithm was developed. It provides significant information for distinguishing trees from lawns and other objects having similar spectral properties.

Common Texture Detection

To evaluate tree textural information, different common texture algorithms were applied and compared in this study. They included local statistical measures (contrast, energy, entropy, homogeneity, and variance), co-occurrence matrix based techniques (also using the same contrast, energy, entropy, homogeneity, and variance), and edge detection algorithms (Sobel, Kirsch, and Canny).

The five local statistical measures are expressed as

$$\text{Contrast:} \quad Con = \sum_{i=0}^{N-1} \sum_{j=0}^{N-1} (i-j)^2 \cdot f(i,j) \tag{1}$$

$$\text{Energy:} \quad Ene = \sum_{i=0}^{N-1} \sum_{j=0}^{N-1} f(i,j)^2 \tag{2}$$

$$\text{Entropy:} \quad Ent = \sum_{i=0}^{N-1} \sum_{j=0}^{N-1} f(i,j) \cdot \log(f(i,j)) \tag{3}$$

$$\text{Homogeneity:} \quad Hom = \sum_{i=0}^{N-1} \sum_{j=0}^{N-1} \frac{f(i,j)}{1+|i-j|} \tag{4}$$

$$\text{Variance:} \quad Var = \frac{1}{N^2} \sum_{i=0}^{N-1} \sum_{j=0}^{N-1} [f(i,j) - \overline{f(i,j)}]^2$$

$$\text{with } \overline{f(i,j)} = \frac{1}{N^2} \sum_{i=0}^{N-1} \sum_{j=0}^{N-1} f(i,j) \tag{5}$$

where $f(i, j)$ is the brightness value of the pixel located at ith row and jth column in the operation window, and N is the pixel number of the operation window.

The co-occurrence matrix based techniques are often employed to detect textural features in remotely sensed images (e.g., Haralick, 1986; Gong *et al.*, 1992; Zhang, 1999). The Sobel, Kirsch, and Canny operators are commonly used edge operators. They can be found in the image processing literature (e.g., Parker, 1997).

Figure 1 shows the original aerial image and some results of commonly used texture operations with a 3 by 3 template. The local variance measure demonstrates a promising result for tree extraction (Figure 1b). Treed areas are highlighted and separated from lawn and other objects having a low variance. Unfortunately, edges of buildings, streets, and shadows are also highlighted, causing confusion with the treed areas. However, the results of local contrast, energy, entropy, and homogeneity measures appear as smoothed images. They are not suitable for tree feature extraction.

Figure 1c illustrates the result of edge detection using the Sobel operator. The results obtained using Kirsch and Canny operators are similar. They are less smooth than those obtained from local variance detection.

Figure 1d illustrates the result of the co-occurrence matrix based texture extraction with the energy measure. The co-occurrence matrix based results with entropy and homogeneity are similar to Figure 1d. But those with contrast and variance are not satisfactory. In the co-occurrence matrix transformation, the inter-pixel distance was 1, the angle was 0°, and the image was reduced to 32 gray levels. It can be seen in Figure 1d that treed areas are highlighted. Unfortunately, lawn areas cannot be suppressed well.

The above results demonstrate that treed areas are poorly detected by using common texture detection algorithms. In comparison to multispectral classification, however, the local variance extraction and edge detection represent an important advantage, i.e., treed areas can be well separated from lawn and other objects with similar spectral properties (compare Figures 1b and 1c with Figure 5c). If the edges of buildings and streets and shadows can be eliminated, treed areas should be extracted well.

A 5 by 5-pixel operation window was also applied to the textural detection using the aforementioned texture measures. Large treed areas were highlighted more smoothly. However, small treed areas were smoothed out and edges of other objects became broader. This could reduce the accuracy of the treed area extraction. Therefore, a 3 by 3 window was adopted in this study for the local statistical measurements.

To eliminate edges of other objects and better detect tree textures, an algorithm of conditional variance detection was developed.

Conditional Variance Detection

The variance in treed areas is usually higher than that in other object areas. Treed areas can be highlighted well by calculating the local variances in an image. However, edges of other objects also have a high local variance. They are highlighted together with the treed areas during the variance calculation (Figure 1b). But, these edges are considered as noise for the purpose of tree extraction.

In order to effectively highlight treed areas and simultaneously suppress noise, an algorithm of conditional variance detection is developed, which consists of a directional variance detection and a local variance detection. The directional variance detector is shown in Figure 2. The function of the directional variance detection is to detect whether the central pixel of the operation window is located in a treed area. If the central pixel is in a treed area, a local variance calculation will be carried out to highlight the pixel. Otherwise, the local variance calculation will be avoided to suppress the pixel. To effectively detect edges of other objects and separate them from treed areas, the size of the operation window for directional variance detection should be larger than the window for local variance calculation.

The directional variance detector first measures the pixel variances along the central lines (shaded pixels in Figure 2) on each side of the central pixel (four directions). The central pixel is then assessed according to the values of the directional variance on each side. When the variance value on one of the four sides is less than a given threshold, it can be concluded that there is a homogeneous area on this side or the central line is along a straight edge. In this case, the central pixel should be located either in a homogeneous area or on a straight edge, but not inside a treed area. Under this condition, the central pixel is regarded as a "non-tree" pixel. It will be assigned a lower value and the local variance calculation will not be carried out. In other cases (conditions), the calculation of the local variance (within a 3 by 3 window) will be carried out and the current pixel will receive a higher value. By adding this control condition, treed areas can be detected and most edges of other objects can be eliminated (Figure 3; compare with Figure 1b).

The four directional variance operator can be described as:

$$DVar = \frac{1}{n} \sum_{i=-n}^{n-1} [f(i,j) - \overline{f(i,j)}]^2$$

$$\text{with } \overline{f(i,j)} = \frac{1}{n} \sum_{i=-n}^{n-1} f(i,j), \text{ and}$$

$$i < 0,\ j = 0, \text{ for the upper side;}$$

$$i \geq 0,\ j = 0, \text{ for the lower side.} \tag{6}$$

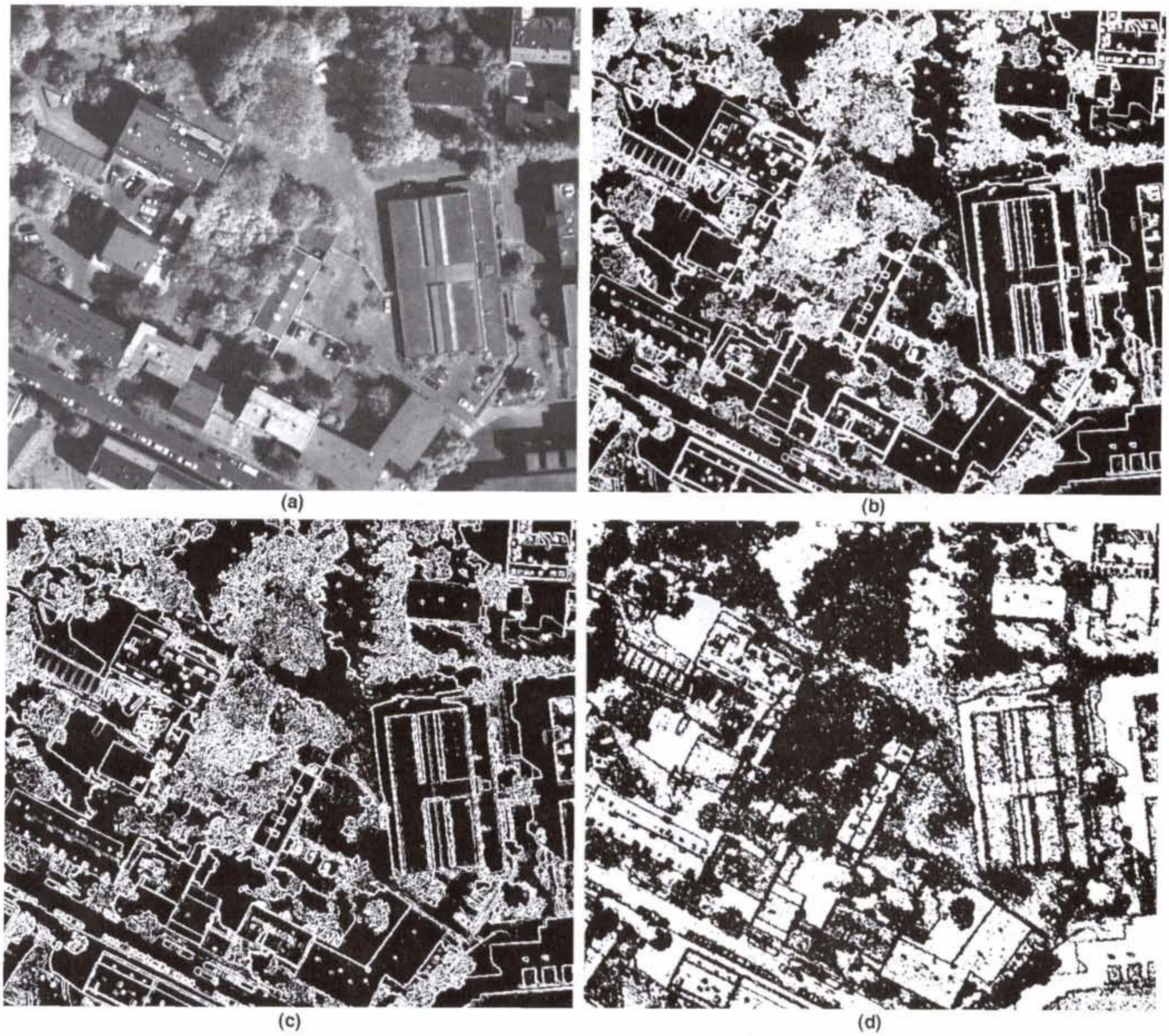

Figure 1. Textural features of urban treed areas detected using common methods with a 3 by 3 window (500- by 450-pixel section, 0.25 m/pixel). (a) Original image (infrared band). (b) Local variance. (c) Edges detected by Sobel operator. (d) Co-occurrence matrix based extraction using the energy measure.

$$
\begin{aligned}
DVar &= \frac{1}{n}\sum_{j=-n}^{n-1}\left[f(i,j)-\overline{f(i,j)}\right]^2 \\
\text{with } \overline{f(i,j)} &= \frac{1}{n}\sum_{j=-n}^{n-1} f(i,j), \text{ and} \\
i &= 0,\ j < 0, \text{ for the left side;} \\
i &= 0,\ j \geq 0, \text{ for the right side.}
\end{aligned} \tag{7}
$$

where *Dvar* is directional variance, $f(i, j)$ is the value of the pixel located at ith row and jth column in the operation window (Figure 2), and n is the pixel count on each side of the central pixel.

The size of the directional variance operation window and the threshold are decided according to the resolution of images and the relationship between the trees and buildings. In this study, the window for directional variance was set to 9 by 9 pixels and the window for local variance was 3 by 3. Because of the wide variety of the edges of other objects, especially building edges, some edge segments still remain after the conditional variance detection. However, the major goals of highlighting treed areas, separating lawn areas from treed areas, and suppressing edges of other objects have been achieved (compare Figure 3 with Figure 1b). This provides the ability to accurately extract urban treed areas by further integrating spectral analysis.

The effect of a directional variance operator with eight directions was also evaluated. The operator with four directions (Figure 2) provides better results.

Treed Area Classification by Integrating Textural and Spectral Features

To further eliminate noise and accurately extract treed areas, a procedure integrating textural and spectral features into an image classification routine was developed. The procedure is briefly described with the flow chart shown in Figure 4.

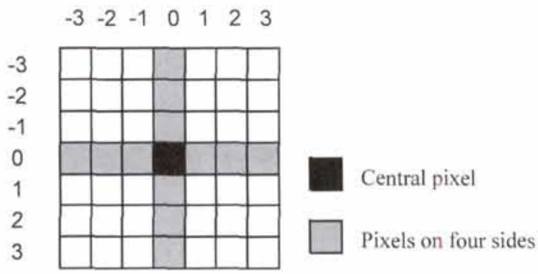

Figure 2. Operation window for calculating the directional variance on each of the four sides.

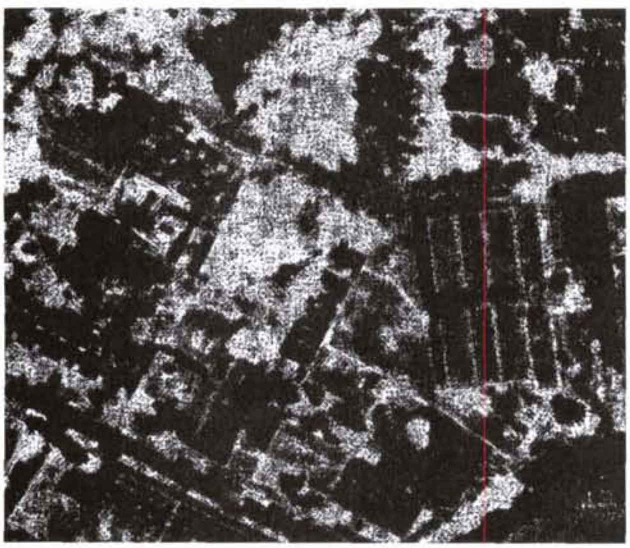

Figure 3. Treed areas highlighted by conditional variance detection (input image: Figure 1a).

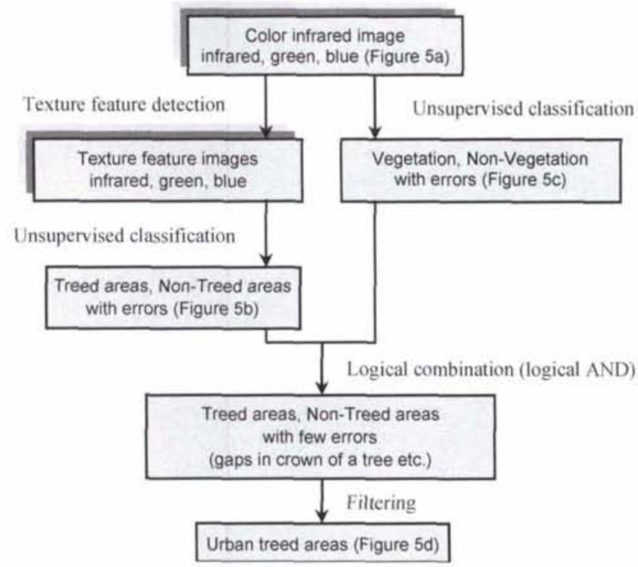

Figure 4. Procedure for treed area extraction using textural and spectral feature integration.

In addition to the infrared band, the green and blue bands were also employed to improve the tree texture detection. The texture information in the infrared band was extracted by using the conditional variance detection. Ideally, the textural information in the blue and green bands should also be detected using the conditional variance detection. However, because the available blue and green bands have a resolution that is two times worse than that of the infrared band (e.g., blue and green: 0.5 m, infrared: 0.25 m; see subsection on Data Used and Study Areas), only the local variance detection was applied to these two bands to avoid the unnecessary reduction in the information of small treed areas. This might reduce the extraction accuracy, but the spectral classification thus followed can compensate for the accuracy reduction to a certain extent, because the elimination of other object edges (noise) in the infrared band changed the color of the edges in the multispectral texture feature image composed of the three texture bands. Of course, if all three bands had the same resolution and the conditional variance detection was applied to all the bands, the accuracy of the texture classified results could be higher.

The three texture feature images (bands) were first smoothed with a 3 by 3 low pass filter and then classified using the ISODATA unsupervised clustering method (ERDAS, 1997). This method is becoming popular in classification of heterogeneous high-resolution images because it is highly successful at finding the spectral clusters that are inherent in the images (e.g., Hahn and Stätter, 1998; Zhang, 1998b). The improvement of treed area detection based on textural information in the three bands is shown in Figure 5b. It can be seen that treed areas are extracted more accurately than by using only one infrared band (Figure 3). Edges of other objects were further eliminated. However, a minor amount of noise still remains.

To further remove this noise, treed areas in the color-infrared image were also classified according to their spectral information by using the ISODATA method (Figure 5c). It is obvious that treed areas cannot be classified properly because lawn areas and some other objects, such as some roofs and cars, present close, even identical, spectral properties. However, edge segments of other objects, which were not eliminated by the conditional variance detection, can be separated from trees and lawn.

Integrating the result of the textural classification with that of the spectral classification, using the logical AND operation, increases the accuracy of treed area extraction. Shadows on tree crowns resulted in a few gaps among the tree crowns. Some cars showing similar textural and spectral properties caused the mislabeling of a few cars as trees. A "spot and gap" filtering, which removes isolated areas according to their sizes (Zhang, 2000), was carried out. After the filtering, the small gaps within tree crowns were added back as trees and the mislabeled cars were eliminated. Unfortunately, some small trees, smaller than the width of a car (about 1.6 m on the ground, or about 8 pixels in diameter in a 0.25-m resolution image and 6 pixels in a 0.3-m image), were also lost. The final result is shown in Figure 5d.

Results and Accuracy Analysis

Data Used and Study Areas

The method developed in this study was applied to classifying treed areas in the cities of Berlin and Duisburg, Germany. Two scenes of high-resolution color-infrared images composed of the

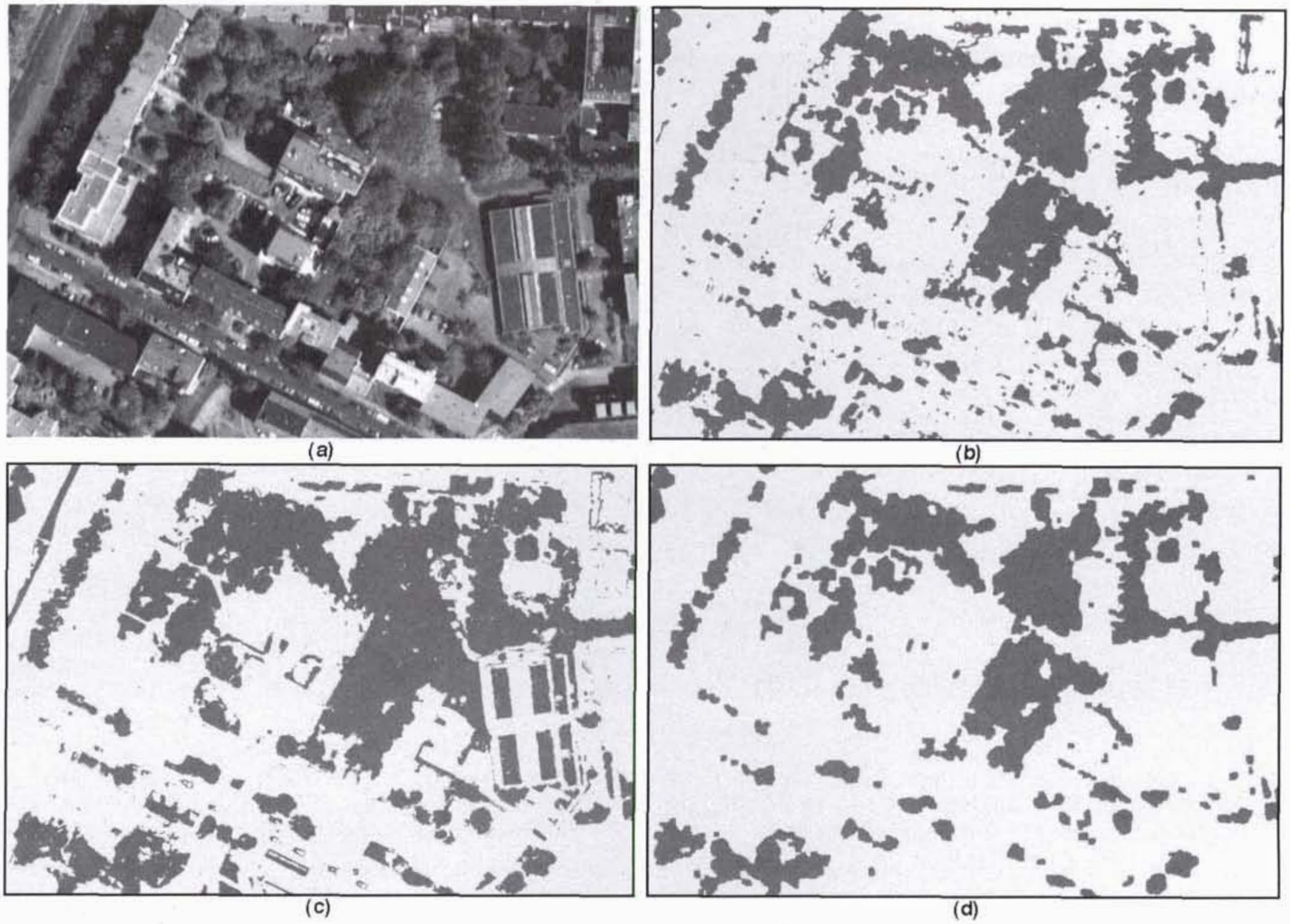

Figure 5. Results of textural and spectral feature integrated classification (750- by 500-pixel section, 0.25 m/pixel). (a) Color-infrared image (here in black and white). (b) Treed areas classified according to their texture information. (c) Treed areas (vegetation) classified according to their spectral information. (d) Final result after logical combining (b) with (c) and after noise filtering.

infrared, green, and blue bands of the HRSC-A sensor—a multispectral and stereo CCD (charge coupled device) line sensor (Wewel *et al.*, 1998)—were employed (Figures 5a and 6a). The data set covering the Berlin area was recorded on 14 May 1998 and that of Duisburg on 01 September 1998. The flight altitudes of both scenes were at about 3000 m. The green and blue bands were recorded with a lower resolution (four pixels to one) due to the storage limitation on board. The data sets were geometrically corrected in the pre-processing. For the Berlin scene, the infrared band was resampled to a resolution of 0.25 m, and the green and blue bands to 0.50 m. For Duisburg, the infrared band was resampled to 0.30 m, and the green and blue bands to 0.60 m.

The study area in Berlin covered approximately 2,100 by 3,500 pixels (0.25 m/pixel). Within the study area, big trees, small trees, bushes, and lawns are located in streets and backyards, between buildings and houses, as well as in open areas. There are many other objects, such as some playgrounds, roofs, and cars, which have spectral properties close to, or even identical to, trees (Figure 5a). The Duisburg scene covered an area of about 1,700 by 3,500 pixels (0.30 m/pixel). The buildings in the area are relatively smaller than those in the Berlin area. In addition, there are many large and small lawn areas located adjacent to trees and buildings (Figure 6a).

Comparison of Extracted Results

Figures 5c and 5d, as well as Figure 6, show the comparison of results classified by the conventional method and the method developed in this study. They demonstrate that conventional multispectral classification is insufficient for the extraction of treed areas in high-resolution multispectral imagery. In particular, lawns and many other objects with similar spectral properties cannot be separated from trees (Figures 5c and 6b). The method developed in this study, however, demonstrated highly accurate results. The treed areas and individual trees were extracted separately from lawns, roofs, and playgrounds having colors similar to trees. In the Duisburg scene, even lawn areas in small backyards (Figure 6c, bottom) were well separated from treed areas. Using traditional multispectral classification, they were extracted simply as vegetation (specifically, tree and lawn). The advantages of the new method are especially obvious in the enlarged sub-areas.

Accuracy Analysis

Accuracy assessment was carried out using the random point method in an area of 1500 by 2000 pixels for Berlin and 1000 by 1500 pixels for Duisburg. Four-hundred randomly selected points were assessed in the Berlin area and 300 randomly

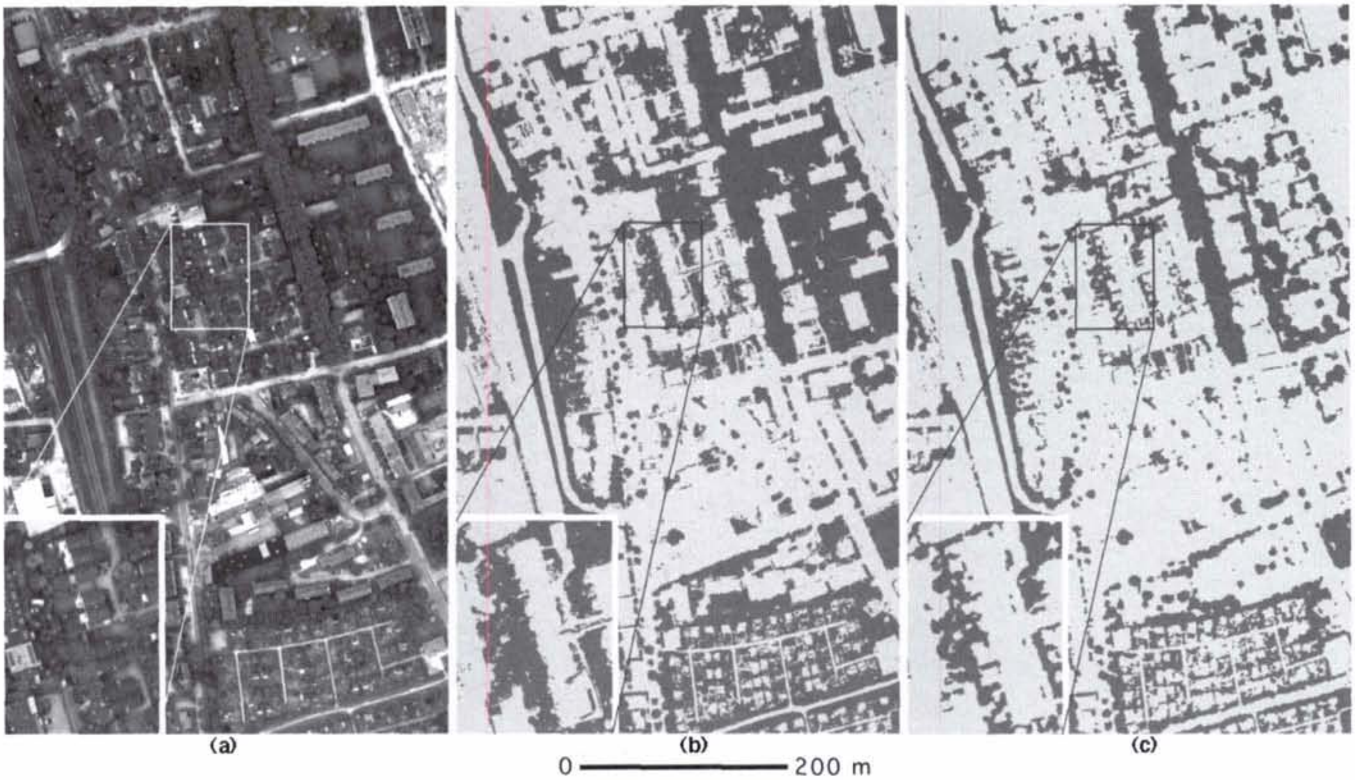

Figure 6. Comparison of tree extraction using a conventional multispectral classification and the textural feature integrated classification in the area of Duisburg (1,500- by 2,300-pixel section, 0.30 m pixel). (a) Color infrared image (here in black and white) as input. (b) Result of a conventional multispectral classification. (c) Result of the textural feature integrated classification.

selected points were assessed in the Duisburg area. The color-infrared images of the HRSC-A sensor were used as visual reference data. The accuracies of the conventional classification and the texture integrated classification are reported in Table 1.

It can be seen in the table that the accuracies of the texture integrated classification are much higher than those of a conventional classification. The user's accuracy and kappa statistics (Richards and Jia, 1999) of the tree class were significantly increased from 61 percent and 0.54, by a multispectral classification, to 97 percent and 0.97 for the Berlin area, respectively. And, they were increased from 73 percent and 0.58 to 94 percent and 0.92 for the Duisburg area. The average user's accuracy of the treed area extraction was increased by almost 30 percent and the average kappa statistics by over 0.35.

Conclusions

It was demonstrated that the conditional variance detection algorithm developed in this study surpasses common texture analysis algorithms for tree texture detection. Further, the texture integrated classification delivered a significant improvement in the extraction of urban treed areas from high-resolution imagery. This new method was applied to treed area extraction from color infrared images with different resolutions, covering different urban areas. In all the cases, it led to a highly accurate result. Treed areas, and even individual trees, can be extracted exactly.

The accuracy of these automatically extracted treed areas is higher than that from the usual manual interpretation. This conclusion is made based on the fact that the minimum mapping unit of a visual interpretation usually is 2 by 2 mm^2 on image hardcopies (McCormick, 1999; Shanghai Remote Sensing Office, 1993). In this study, treed areas with a minimum unit of about 2 by 2 m^2 or less on the ground were extracted from images with a resolution of 0.3 m. For a visual interpretation, however, an image hardcopy or photo usually contains a resolution of more than 5 pixels/mm. Thus, a 2 by 2 mm^2 mapping unit on such image hardcopy is larger than 3 by 3 m^2 on the ground.

Because the approach developed is based on the analysis of textural and spectral characteristics within a local operation window, the effects of canopy closure, shadow, and sun angle were not taken into account. Optimum results will be achieved when the color-infrared imagery is taken during the growing season and when the sun angle is high (about noon). Otherwise, the accuracy will be reduced depending on the degree of canopy closure and the depth of shadow cover. This is also true for a visual interpretation.

Table 1. Accuracy of the Treed Areas Classification Using a Conventional Spectral Method and the New Spectral-Texture Method

	Multispectral classification		Texture integrated classification	
	User's Accuracy (%)	Kappa Statistics	User's Accuracy (%)	Kappa Statistics
Berlin	61	0.54	97	0.97
Duisburg	73	0.58	94	0.92

Acknowledgments

The research was done at the German Aerospace Center (DLR). It is with great appreciation that I thank Mr. F. Lehmann, Institute of Space Sensor Technology and Planetary Exploration, DLR, for his support during the research.

References

Anys, H., A. Bannari, D.C. He, and D. Morin, 1994. Texture Analysis for the Mapping of Urban Areas Using Airborne MEIS-II Images, *Proceedings of the First International Airborne Remote Sensing Conference and Exhibition (III)*, 11–15 September, Strasbourg, France, pp. 231–245.

Barnsley, M.J., and S.L. Barr, 1996. Inferring Urban Land Use from Satellite Sensor Images Using Kernel-Based Spatial Reclassification, *Photogrammetric Engineering & Remote Sensing*, 62(8):949–958.

Bruniquel-Pinel, V., and J.P. Gastellu-Etchegorry, 1998. Sensitivity of Texture of High Resolution Images of Forest to Biophysical and Acquisition Parameters, *Remote Sensing of Environment*, 65:61–85.

Brunn, A., and U. Weidner, 1997. Extracting Buildings from Digital Surface Models, *International Archives of Photogrammetry and Remote Sensing*, 17–19 September, Stuttgart, Germany, 32(Part 3-4W2): http://www.ipb.uni-bonn.de/ipb/lit/lit.html#1997.

Coops, N., and D.S. Culvenor, 2000. Utilizing Local Variance of Simulated High Spatial Resolution Imagery to Predict Spatial Pattern of Forest stands, *Remote Sensing of Environment*, 71:248–260.

Culvenor, D.S., N. Coops, R. Preston, and K. Tolhurst, 1999. A Spatial Clustering Approach to Automated Tree Crown Delineation, *Proceedings of the International Forum on Automated Interpretation of High Spatial Resolution Digital Imagery for Forestry*, 10–12 February, Victoria, BC, Canada, Natural Resources Canada, Canadian Forest Service, Pacific Forestry Centre, pp. 67–80.

Dreyer, P., 1993. Classification of Land Cover Using Optimized Neural Nets on SPOT Data, *Photogrammetric Engineering & Remote Sensing*, 59:617–621.

ERDAS, 1997. *ERDAS Field Guide, Fourth Edition*, Atlanta, Georgia, 656 p.

Gao, J., and D. Skillcorn, 1998. Capability of SPOT XS Data in Producing Detailed Land Cover Maps at the Urban-Rural Periphery, *International Journal of Remote Sensing*, 19(15):2877–2891.

Gong, P., and P.J. Howarth, 1990. The Use of Structural Information for Improving Land-Cover Classification Accuracies at the Rural-Urban Fringe, *Photogrammetric Engineering & Remote Sensing*, 56(1):67–73.

Gong, P., D.J. Marceau, and P.J. Howarth, 1992. A Comparison of Spatial Feature Extraction Algorithms for Land-Use Classification with SPOT HRV Data, *Remote Sensing of Environment*, 40:137–151.

Gougeon, F.A., 1995. A Crown-Following Approach to the Automatic Delineation of Individual Tree Crowns in High Spatial Resolution Aerial Images, *Canadian Journal of Remote Sensing*, 21(3):274–284.

Haala, N., C. Brenner, and K.-H. Anders, 1998. 3D Urban GIS from Laser Altimeter and 2D Map Data, *International Archives of Photogrammetry and Remote Sensing*, 32(Part 3/1):339–346.

Hahn, M., and C. Stätter, 1998. A Scene Labeling Strategy for Terrain Feature Extraction Using Multisource Data, *International Archives of Photogrammetry and Remote Sensing*, 32(Part 3/1): 435–441.

Haralick, R.M., 1986. Statistical Image Texture Analysis, *Handbook of Pattern Recognition and Image Processing* (T.Y. Young and K.-S. Fu, editors), Academic Press, Orlando, Florida, pp. 247–279.

Hildebrandt, G., 1996. *Fernerkundung und Luftbildmessung: für Forstwirtschaft, Vegetationskartierung und Landschaftsökologie*, Wichmann, Heidelberg, 676 p.

Marceau, D.J., D.J. Gratton, R.A. Fournier, and J.P. Fortin, 1994. Remote Sensing and the Measurement of Geographical Entities in a Forested Environment. 2. The Optimal Spatial Resolution, *Remote Sensing of Environment*, 49(2):105–117.

McCormick, C.M., 1999. Mapping Exotic Vegetation in the Everglades from Large-Scale Aerial Photographs, *Photogrammetric Engineering & Remote Sensing*, 65(2):179–184.

Nowak, D.J., R.A. Rowntree, E.G. McPherson, S.M. Sisinni, E.R. Kerkmann, and J.C. Stevens, 1996. Measuring and Analyzing Urban Tree Cover, *Landscape and Urban Planning*, 36:49–57.

Parker, J.R., 1997. *Algorithms for Image Processing and Computer Vision*, John Wiley & Sons, New York, N.Y., 417p.

Pinz, A., 1999. Tree Isolation and Species Classification, *Proceedings of the International Forum on Automated Interpretation of High Spatial Resolution Digital Imagery for Forestry*, 10–12 February, Victoria, BC, Canada, Natural Resources Canada, Canadian Forest Service, Pacific Forestry Centre, pp. 127–139.

Richards, J.A., and X. Jia, 1999. *Remote Sensing Digital Image Analysis, An Introduction, Third Edition*, Springer-Verlag, Berlin, Heidelberg, Germany, 363 p.

Shanghai Remote Sensing Office, 1993. *Multiple Environment Investigation in the City of Shanghai by Means of Aerial Remote Sensing*, Shanghai News Publishing House, Shanghai, 170 p. (in Chinese).

St-Onge, B.A., and F. Cavayas, 1997. Automated Forest Structure Mapping from High Resolution Imagery Based on Directional Semivariogram Estimates, *Remote Sensing of Environment*, 61:82–95.

Wewel, F., F. Scholten, G. Neukum, and J. Albertz, 1998. Digitale Luftbildaufnahme mit der HRSC-Ein Schritt in die Zukunft der Photogrammetrie, *Photogrammetrie-Fernerkundung-Geoinformation (PFG)*, 6:337–348.

Woodcock, C.E., and A.H. Strahler, 1987. The Factor of Scale in Remote Sensing, *Remote Sensing of Environment*, 21:311–332.

Wulder, M., K.O. Niemann, and D.G. Goodenough, 2000. Local Maximum Filtering for the Extraction of Tree Locations and Basal Area from High Spatial Resolution Imagery, *Remote Sensing of Environment*, 73:103–114.

Zhang, Y., 1998a. *Aufbau eines auf Satellitenfernerkundung basierten Informationssystems zur städtischen Umweltüberwachung: Das Beispiel Shanghai*, PhD dissertation, FU Berlin, Berliner Geowissenschaftliche Abhandlung, Reihe C, Band 17, 140 p.

———, 1998b. Detection of Urban Housing Development Using Multisensor Satellite Data and Maps, *International Archives of Photogrammetry and Remote Sensing*, 32(Part 3/1):292–299.

———, 1999. Optimisation of Building Detection in Satellite Images by Combining Multispectral Classification and Texture Filtering, *ISPRS Journal of Photogrammetry and Remote Sensing*, 54:50–60.

———, 2000. A Method for Continuous Extraction of Multispectrally Classified Urban Rivers, *Photogrammetric Engineering & Remote Sensing*, 66(8):991–999.

(Received 09 February 2001; accepted 28 June 2001; revised 03 August 2001)